Acousto-optic architectures for multidimensional phased-array antenna processing

Riza, Nabeel

Nabeel A. Riza, "Acousto-optic architectures for multidimensional phased-array antenna processing," Proc. SPIE 1476, Optical Technology for Microwave Applications V, (1 August 1991); doi: 10.1117/12.45569

SPIE.

Event: Orlando '91, 1991, Orlando, FL, United States

ACOUSTO-OPTIC ARCHITECTURES FOR MULTI-DIMENSIONAL PHASED ARRAY ANTENNA PROCESSING.

by
Nabeel A. Riza
General Electric Corporate R & D Center
P. O. Box 8, Schenectady, N.Y. 12301

Abstract

In-line additive acousto-optic architectures for linear and planar phased arrays are described for one dimensional (1-D) and two dimensional (2-D) beam scanning, respectively, along with a simultaneous multiple beam forming architecture. A transmission mode acousto-optic processor is demonstrated in the laboratory. Electronic and optical receive mode systems are described.

1. Introduction

Recently, there has been interest in using optical techniques for signal generation, reception, and control of phased array antennas. Optical fibers for true time delay beam steering have been proposed, and phase based antenna beam forming systems have also been suggested [1,2]. Earlier, we introduced and experimentally demonstrated an efficient 1-D in-line additive acousto-optic (AO) architecture for signal generation and reception in linear phased array antennas operating in the lower microwave bands (up to 6 GHz) [3,4]. This phase based antenna beam scanning AO architecture eliminates all the microwave phase shifters and power dividers required in a typical electronically controlled phased array antenna. The system uses two acousto-optic devices (AODs), where each AOD simultaneously performs the dual function of generating the microwave signal and controlling the signal phase. Only one control signal is required for positioning the antenna beam at a desired scan angle. In this paper, the basic in-line additive architecture for a linear phased array antenna is extended to provide 1-D and 2-D beam scanning for multiple linear arrays and planar arrays, respectively [4]. The in-line additive architecture can also be adapted to produce simultaneous multiple beams in space We describe a N beam formation architecture that uses a N channel acousto-optic device and an array of N laser diodes. Experimental results are described for the linear array architecture.

2. Basic Phased Array Antenna Theory

An array antenna consists of a number of individual radiating elements placed at a suitable distance with respect to each other. The relative amplitude and phase of the signals driving the individual antenna elements are externally controlled to generate a particular antenna beam pattern resulting from a sum of all the array radiating elements. A linear array consists of antenna elements arranged along a straight line. This type of array can be used to provide broad coverage in one direction and narrow beamwidth in the orthogonal direction. For analysis purposes, we shall consider a linear array of N elements equally spaced a distance **a** apart, with each element equivalent to an isotropic point source (sink) radiating (receiving) uniformly in all directions. The array antenna can be a transmitting antenna, and via the reciprocity principle of electromagnetics, the same array can be considered as a receiving antenna. In order to transmit energy at an angle θ_0 with respect to the array normal direction, the plane wave interference condition requires that the phase difference of signals driving adjacent elements be $\alpha=2\pi(a/\lambda)\sin\theta_0$,where λ is the radiated wavelength [5]. Thus, the adjacent antenna elements in the array are driven by signals satisfying this phase condition. The amplitudes of these signals can be suitably selected to yield desired beam shapes. Each individual antenna radiates its own pattern, and the combined far field radiation observed at an angle θ is the sum of all the individual radiation patterns due to all the elements in the array. The main beam of the far-field radiation pattern can be rotated by varying the phase difference α of the signals driving the array antennas. This is the principle for phase based beam steering antenna arrays. Note that in order to prevent grating lobes from appearing over the antenna beam scan width, the antenna element spacing

 0-8194-0585-X/91/$4.00

has to be of the order of half the carrier wavelength. In addition, unlike true time delay beam steering, the antenna instantaneous bandwidth is limited to a few percent of the carrier frequency to prevent beam squinting. Nevertheless, for most radar applications, phase based beam steering can be applied to array antennas [6].

3. The Basic AO Architecture for a Linear Phased Array Antenna

Fig.1 shows the basic AO architecture used for generating the necessary signals for beam formation and beam scanning in linear phased arrays. The processor consists of two AOD's, a high speed detector array or a linear fiber-detector array, a coherent light source, imaging and Fourier transforming optics, and two signal generators to provide the antenna carrier and control frequency signals, respectively. The signals $s_1(t)$ and $s_2(t)$ are fed into AOD1 and AOD2, respectively, where $s_1(t)=a\cos\omega_c t$, and $s_2(t)=a\cos(\omega_c+\omega_o)t$. ω_c is the center angular frequency of the AOD's and ω_o is the control angular frequency for steering the array antenna beam. Light from the laser, after being collimated along the x direction and focussed along the y direction, is incident at the Bragg angle in AOD1. The undiffracted DC and +1 diffracted order from AOD1 is 1:1 imaged on to the acoustic column in AOD2 such that the DC light from AOD1 is Bragg matched to AOD2. This results in a -1 diffracted order from AOD2, while the +1 order from AOD1 passes through AOD2 essentially unaffected. These almost collinear +1 and -1 diffracted order beams from AOD1 and AOD2, respectively, are imaged on to a fiber-detector array after an M times magnification. The DC light is blocked in the Fourier plane of AOD2. The intensity at the detector plane can be written as

$$I(x,t)\propto\left|E(x,t)\right|^2=\text{Constant Bias}+G_0\cos\left[(2\omega_c+\omega_0)t-(\omega_0/Mv_a)x\right], \tag{1}$$

where Constant Bias= $a^2/2$, $G_o=a^2/2$, and v_a is the acoustic signal velocity in the AOD's. The above expression consists of a uniform bias term, and a signal term with both temporal and spatial modulation. Recall from our discussion on phased array beam steering that phase based beam steering requires a set of antenna drive signals on the antenna temporal carrier with appropriate phase values. The above expression shows that we can obtain this set of antenna drive signals by simply using a fiber/detector array to appropriately sample the phase distribution of the temporally varying intensity pattern . In the case of uniform linear phase sampling, the detectors are placed at an equal distance **d** from each other. The signal generated at the n^{th} detector after spatial integration over the detector photo-sensitive area d_x x d_y is amplified by a microwave amplifier. If the spatial period of the intensity pattern is much greater than the sampling direction detector size, that is, $u_x d_x << 1$ where $u_x= f_o/Mv_a$ is the spatial frequency generated along the detector array, and d_x is the width of the detector along the sampling x direction, then the signal produced by the n^{th} detector can be approximated as

$$i_n(t)\approx G\cos\left[(2\omega_c+\omega_0)t-n\,\omega_0 d/Mv_a\right], \tag{2}$$

where the bias term has been dropped, $G=0.5G_o\,d_x\,d_y$, n=0,1,2,....., N−1 and N is the total number of detectors used in the linear sampling array. Note that Eqn.3 gives the drive signal that is fed to the n^{th} antenna in a uniform linear phased array for achieving beam steering. This signal can be expressed as $i_n(t) = G\cos(\omega t - n\varphi)$, where the antenna carrier angular frequency is $\omega = 2\omega_c+\omega_o$,and the phase difference between signals in adjacent antennas in the array is $\varphi= \omega_o d/Mv_a$. From phased array antenna theory, recall that to position the antenna beam at an angle $\theta=\theta_o$, we would require $\varphi= \alpha + m\,2\pi$ where m=0, ±1,..... Using the expressions for α and φ, the design equation for the optical processor to achieve a beam position θ_o for a control frequency f_o is:

$$\theta_0=\sin^{-1}\left\{(a/\lambda)\left[f_0\,d/Mv_a-m\right]\right\}. \tag{3}$$

Note that the same angle θ_o can be obtained for different values of the frequency f_o corresponding to different values of m. Also recall that as we are using the phase shift beam steering technique, accurate beam pointing requires the antenna instantaneous microwave bandwidth to be less than a few percent (2%) of the antenna carrier frequency [7]. This implies that $\Delta f_o/f' << 1$ where Δf_o is the maximum control frequency change required for the maximum beam scan angle and f' is the antenna carrier center frequency, where $f'=2f_c + \Delta f_o/2$. Note that each beam scan angle position corresponds to a different antenna carrier frequency, implying that the beam positions are frequency coded. This could allow for secure communications. If the transmitted antenna carrier frequency f' has to be independent of the control frequency f_o, two kinds of oscillators are required for this system. One oscillator is a RF signal generator providing the scan control frequency f_o, while the other is a microwave oscillator operating at half the desired antenna carrier frequency (also equal to the AOD center frequency). The two signals are mixed together in a microwave mixer giving $s(t)=2a \cos(\omega_o t) \cos(\omega_c t)$, which is equal to $s(t)= a \cos(\omega_o + \omega_c)t + a \cos(\omega_o - \omega_c)t$. This signal is split by a microwave power divider into two paths. One path goes through an upper sideband filter giving the microwave signal $s_1(t)= a \cos(\omega_c + \omega_o)t$ that is fed to AOD1. The other path goes to a lower sideband filter giving the signal $s_2(t)= a \cos(\omega_c - \omega_o)t$ that is used to drive AOD2. The single sideband filtering can also be done optically by using spatial filtering in the Fourier planes of AOD1 and AOD2, respectively. In this case, the signal generated by the n^{th} detector is

$$i_n(t) \approx G \cos\left[2\omega_c t - n\omega_0 d / M v_a\right]. \tag{4}$$

Note that the antenna carrier frequency stays fixed at $2\omega_c$ and is independent of the scan control frequency ω_o. This architecture can be applied to **intrapulse beam forming** when transmitting long wideband signals. In this case, when ω_c is changed with time, ω_o is independently and simultaneously adjusted to continue pointing the beam at the desired angle. Beam scanning can also be achieved by **frequency scanning**. In this case, ω_o is fixed to give a constant inter-antenna element phase value, while the carrier is scanned by scanning the frequency ω_c.

4. Experimental Demonstration of the Basic AO Architecture

The AO technique is tested at RF for an antenna carrier frequency of 120 MHz using two tellurium dioxide Bragg cells with a 70 μsec time aperture, 60 MHz center frequency, and a 30 MHz bandwidth. The optics used consists of a 20cm collimating spherical lens, a 30cm focussing cylindrical lens for AOD1, 20cm spheres for 1:1 imaging, 25cm and 30cm spheres for imaging and Fourier plane filtering, and a 7.5cm spherical lens for the magnification system The N element high speed detector array is simulated by using 2 detectors mounted on x-y micrometer translation stages, allowing for the detector spacing **d** to be adjusted according to design specifications, while placing the detectors at any position along the focussed slit of light. The specifications for the detector\amplifier set were a high speed UDT PIN-HR008 photo diode detector with a 3nsec max rise time, 200 μm diameter, and responsivity of .33 A/W at 514nm, and a high speed UDT amplifier with 3 dB bandwidth of 500KHz to 400MHz, and transimpedance gain 3.5 X 10^3 Volts/Amp. As the Bragg cell acts as a beam deflector with a finite number of deflected spots, the control frequency is discretized and written as $f_o=p\delta f_o$, p=0,1,2,...., and $\delta f_o=1/T_a$, where T_a is the illuminated Bragg cell aperture. The design for the processor was chosen as δf_o =14.29KHz, v_a=.617mm/μsec, M=4.17, Bragg cell center frequency f_c =60MHz, and a 514 nm Argon ion laser light source. Fig.2 shows the varying phase difference between the two signals generated from the detector pair positioned with a certain interdetector distance **d**. Here, the control frequency is varied to obtain a zero to 2π phase shift for the generated carrier signals. As expected, the experimental plots for phase change .vs. control frequency change shows a linear relationship (See Fig.3).

How fast we switch a beam from one angular position to another depends on how quickly all the detectors provide steady state correctly phased antenna drive signals. Although the proposed phased array antenna optical processor has a parallel signal feed format, the individual signal generation is based on a series fed structure, similar to a 1-D end fed array of total length **X**. The array signal generation is based on the interaction between the two counter propagating acoustic signals in the two AOD's and the light carrier. Assuming that a length X of the two respective AOD's is illuminated with Bragg matched light beams, it takes $X/2v_a$ seconds for the two acoustic signals to cross, and X/v_a seconds for complete interaction between the two signals to occur. At this stage, all the detectors are illuminated by the acoustically modulated light signals, and phased signals are being generated for the radiating antennas. Thus, the processor frequency response depends on the Bragg cell fill time given by $T_a = X/v_a$. T_a is also called the array fill time and affects the transient response of the antenna when the transmitted pulse width T_p is of the order of the array fill time.

5. Simultaneous Multiple Beam Forming AO Architecture

The AO processor can be used to continuously scan the antenna beam over a wide angular region. For continuous beam scanning, a piece-wise linear FM signal is fed to the AOD. Fig.4 shows the AO system that forms N simultaneous arbitrary beams in space. The system is similar to the single beam generation system, except the single laser source is replaced by a laser diode array of N mutually incoherent sources, and the second AOD is replaced by a N channel AOD corresponding to the N beams. The side view of the system shows that light from all the sources interacts with the first single channel AOD, while there is a 1:1 source to channel mapping in the multichannel AOD (MCAOD); i.e., the p^{th} laser diode light interacts only with the p^{th} channel in MCAOD. The signal fed to the first AOD is $s_1(t)=a\ \cos\omega_c t$, while the signal fed to the p^{th} channel of the MCAOD is $s_p(t)=a_p\ \cos(\omega_c+\omega_p)t$ where ω_p is the control frequency required to produce the p^{th} beam at a scan angle θ_p. A combination of spherical and cylindrical lenses at the output of the processor integrates the light from different, spatially multiplexed channels in the MCAOD on to the 1-D detector array, giving a sum of individual light intensities from each source; i.e., the light from the n^{th} detector in the linear detector array is:

$$i_n(t) = \sum_{p=1}^{N} I_p(n) \quad + \text{Constant Bias}, \tag{5}$$

where $I_p(n)= G_p \cos[\ (2\omega_c+\omega_p)t - n\varphi_p\ ]$ and φ_p is the required phase shift to position a beam at angle θ_p to broadside. Thus, $i_n(t)$ gives the required N signals needed to simultaneously generate N beams at scan angles $\theta_1,.....,\theta_p,.....,\theta_N$, respectively. Currently available 32 channel MCAOD's can be used in this system to provide a maximum of 32 simultaneous beams in space.

Simultaneous beams pointing at the same scan angle but on different antenna carrier frequencies can be generated by the multichannel AOD processor. As the phase sampling concept is periodic with 2π radians, a similar phase increment can be obtained for a periodic increment in the control frequency, where m corresponds to the periodic increment in the control frequency. For instance, control frequencies f_1 and f_2 corresponding to m=0,1, respectively, give two beams at the same scan angle θ_o. This approach can give the antenna a multi-frequency operation mode. In addition, multi-frequency operation can also be achieved by a similar architecture (like Fig.4) that uses lenslet arrays and two MCAODs to produce widely spaced carrier frequencies over the radar bands. In this case, because the carrier frequency and carrier phase can be independently controlled (See Eqn.4), and AODs can have wide bandwidths, ω_c can easily be varied to change the antenna carrier frequency.

6. The Electronic and Optical Receive Techniques

The **electronic** phased array antenna receive technique is shown in Fig.5, along with the transmitter part of the system. This receiving system discriminates the angle, range, and doppler information of targets in the radar search range by processing target return signals from the array antenna elements.

The basis of the postprocessing involves reusing the optically generated array transmit signals to cancel the phase factors associated with the received signals from the individual antenna elements, thus generating in phase signals from all the individual returns. For target detection at a scan angle θ_0 to broadside, we transmit a pulse $p_T(t)$ of RF energy of duration T on a carrier frequency $2\omega_c + \omega_o$, with appropriate phase φ_0 set by the optical processor. The signal driving the n^{th} antenna in the phased array is:

$$i_n(t) = p_T(t) G \cos[(2\omega_c + \omega_0)t - n\varphi_0]. \tag{5}$$

After transmitting the radar pulse, the antenna is operated in the receive mode. The return signal at the n^{th} antenna from a target at θ_0 to broadside is approximately given by [8]:

$$i_n(t') = p_T(t') G_{TR}(n) \cos[(2\omega_c + \omega_0 + \omega_d)t' - n\varphi_0], \tag{6}$$

where $p_T(t')$=rect (t'/T), $t'=t-\tau_R$, τ_R= Range Delay=2R/c and ω_d is the Doppler Frequency where ω_d= -2R [dR/dt] $(2\omega_c + \omega_o)/c$. R is the target range for a monostatic system, and $G_{TR}(n)$ is the signal gain dependent on target properties such as radar cross section. The signal in Eqn.6 is a time delayed, frequency shifted replica of the signal transmitted by the n^{th} antenna in the array. Here we have assumed that the pulse width T is much greater than the maximum interantenna element time delay; i.e., T >> Na/c and the doppler frequency satisfies the condition $\omega_d << 2\omega_c + \omega_o$. The received signals are amplified and then mixed with their corresponding transmitter signals. The output of the mixer consists of a low frequency doppler signal without the phase term $n\varphi_0$, and a high frequency signal. The high frequency signal is filtered out by the low pass filter, and the output of the n^{th} T/R module filter is approximately given by:

$$i_n(t') \approx p_T(t') G(n) \cos(\omega_d t'). \tag{7}$$

Note that this signal has a T second time duration with a time delay with respect to the reference transmit time t=0. Also, all the signals from the different T/R modules are in phase. Next, these in phase signals are added up to maximize the receiver output signal-to-noise ratio, giving the signal:

$$i(t') = \sum_{n=0}^{N-1} i_n(t') = N G \cos(\omega_d t'), \tag{8}$$

where we assumed constant amplitude G for all the T/R signals. This output signal contains the necessary range and doppler (motion) information of the detected target at the preset scan angle θ_0. This receiving system can also be used to form a simultaneous multiple target tracking system by using the MCAOD architecture to provide the simultaneous transmit/receive beams to form the multichannel receiver. This receiver is needed when simultaneous multiple beams in space are required to track a fast moving target.

An alternative simultaneous multiple beam receiver is shown in Fig.6 [4,8].The MCAOD system produces the simultaneous multiple transmit beams, while a 2-D space integrating **optical** spectrum analyzer using a MCAOD forms the simultaneous multiple receive beams. The radar return signals from the antenna array elements are heterodyned to the intermediate frequency (IF) ω_c by mixing each antenna signal return with the transmitter's coherent oscillator at ω_c. The output of the mixer is passed through a bandpass filter centered at ω_c that allows only the lower sideband at ω_c to pass through to the channel of the MCAOD in the receiver. The light diffracted by the radar returns in all the spatially multiplexed AOD channels is Fourier transformed by a spherical lens, and the output is read by a 2-D CCD array. Note that the CCD output spatial peak coordinates are related to the target's doppler frequency and angular position [8]. The processor performance for multitarget scenes is

limited mainly by the degree of signal crosstalk and sidelobe contributions of the different target returns in the output frequency plane of the processor.

7. AO Architectures for Planar Arrays

The basic AO architecture (shown in Fig.1) for a linear phased array antenna can be extended to provide 1-D and 2-D beam scanning for planar arrays.

7.1 Multiple Linear Array Feed Architecture for 1-D Scanning

When a pencil beam has to be scanned in one direction, the multiple linear array feed architecture shown in Fig.7 can be used. Instead of focussing the light as a thin slit on the detector/fiber sampling array at the output of the linear array processor,the light is spread out along the direction orthogonal to the detector array. This allows additional sampling detector/fiber arrays to be placed at the enlarged light spatial sampling plane. Note that the spatial frequency along the sampling direction is unaffected by the modification, producing identical signals along a particular sampling position. This allows the optical processor to be used to simultaneously feed multiple linear arrays of antennas without requiring microwave M-way power splitters.

7.2 Architectures for 2-D Scanning using 1-D AODs

Independent antenna beam height and azimuth control (or 2-D scanning) for a planar phased array can be achieved by using 1-D AODs in a crossed Bragg cell configuration. Fig.8 shows an efficient 4 AO cell architecture for 2-D scanning. The cylindrical lens C1 focusses the light along the acoustic column of AOD1. This AOD is Bragg matched to produce a +1 order. The DC and +1 order from AOD1 are spatially separated by the lens S1, forming two separate vertical slits of light. The orthogonally oriented AOD2 and AOD3 are positioned such that the DC and +1 order slits from AOD1 fall within AOD2 and AOD3 acoustic columns, respectively. AOD2 is Bragg matched such that the DC from AOD1 generates a -1 order from AOD2. The undiffracted light from AOD2 is blocked in the plane of AOD4. Similarly, AOD3 is Bragg matched such that the +1 order from AOD1 generates a +1 order from AOD3. The undiffracted light from AOD3 is blocked in the plane of AOD4. The lens S2 focuses the diffracted and undiffracted orders from AOD2 and AOD3 into vertically separated horizontal slits. The acoustic column of AOD4 is placed such that it encloses the horizontal slit from the diffracted orders from AOD2 and AOD3. The other horizontal slit from the undiffracted light from AOD2 and AOD3 is blocked. The -1 order from AOD2 is used to generate a -1 order from AOD4, while the +1 order from AOD3 passes essentially uneffected through AOD4. The two beams, that is the DC beam through AOD4 (which is also the +1 order from AOD3), and the -1 order from AOD4, are interfered on a 2-D detector/fiber array that in-turn feeds a 2-D planar array. AOD1 and AOD4 independently control the antenna beam scanning in one direction, while AOD2 and AOD3 control the beam scanning in the other (orthogonal) direction. Note that this architecture makes efficient use of the light from the diffracted/undiffracted beams. The microwave signals feeding the different AODs are

$$s_{aod\,1} = \cos(\omega_c + \omega_1)t \quad , s_{aod\,4} = \cos(\omega_c - \omega_1)t \quad , s_{aod\,2} = \cos(\omega_c - \omega_2)t \quad , s_{aod\,3} = \cos(\omega_c + \omega_2)t \,. \tag{9}$$

These signals can be generated by mixing the RF control signals with the microwave carrier. The intensity incident at the 2-D fiber array can be expressed as

$$I(x, y, t) \propto \text{Constant Bias} + \cos\left[4\omega_c t - (2\omega_1 / M v_a)x - (2\omega_2 / M v_a)y\right], \tag{10}$$

where $4\omega_c$ is the antenna carrier and ω_1 and ω_2 are the independent beam scan control parameters for the two beam scanning directions. By sampling this intensity pattern with a 2-D detector/fiber array, we can generate the appropriate signals for independent 2-D scanning for a planar array.

Fig.9 shows an alternate architecture for 2-D beam scanning that uses 2 crossed AO cells, thus giving higher overall optical efficiency. In this approach, the antenna carrier frequency varies with the scan angle and the output intensity at the 2-D fiber/detector array is given by

$$I(x,y,t) \propto \text{Constant Bias} + \cos\left[(2\omega_c + \omega_1 - \omega_2)t - (\omega_1 / M v_a)x - (\omega_2 / M v_a)y\right]. \quad (11)$$

The architecture in Fig.9 is a Mach-Zehnder interferometer. The light from a laser is split 50:50 by a beam splitter BS1. Bragg matched light incident on AOD1 produces a +1 order beam that is deflected along the x direction. The mirror M1 is rotated to cancel the deflection along the x direction due to the carrier signal (with zero control frequency) such that the +1 order is normally incident on the combining beam splitter BS2. BS1 and the mirror M2 are tilted to cancel the vertical deflection along the y direction of the -1 diffracted order from AOD2 such that it also strikes BS2 at normal incidence. By cancelling the carrier induced deflections of the +1 and -1 orders along the x and y directions, respectively, the two beams appear collinear at the output ports of BS2. The signals driving the AODs are

$$s_{aod\,1} = \cos(\omega_c + \omega_1)t \qquad , s_{aod\,2} = \cos(\omega_c - \omega_2)t \quad . \quad (12)$$

and ω_1 and ω_2 are the control parameters for 2-D beam scanning.

7.3 Architecture for 2-D Scanning using 2-D AO Cells

Independent radar beam height and azimuth control for a planar phased array radar may be obtained by using two single element, 2-D acousto-optic laser beam deflectors [9]. In these 2-D AO cells, the xy diffracted beam's coordinates are controlled by the frequency of the two signals fed to the orthogonally oriented AO cell transducers bonded to a single 2-D AO crystal. The proposed architecture using the 2-D AO cells is shown in Fig.10. The laser beam is incident at 2-D Bragg angle at the first 2-D AO cell, producing a DC beam, an x position diffracted beam, a y position diffracted beam, and the desired xy position diffracted beam on an upshifted (positive) doppler. The x and y position beams are blocked in the Fourier plane, while the DC beam is 2-D Bragg matched to the second similarly oriented 2-D AO cell producing diffracted beams that includes a down-shifted (negative) doppler xy beam. Note that the xy diffracted beams from the two 2-D AO cells are almost collinear, and are expanded before being interfered at the 2-D fiber/detector plane. In effect, we have two plane waves interfering at the output plane, with the angles between the plane waves controlled independently by the difference in the AOD frequencies driving the similarly oriented channels in the 2 cells. The relative deflection between the xy diffracted orders along the x and y directions controls the azimuth and height angles of the phased array radar pencil beam.

8. Extensions of the Linear Phase Sampling Format

8.1 Non-Uniform Sampling

So far, the spatial phase pattern at the output plane of the processor was uniformly sampled along the linear dimension, i.e., the samplers (fibers/detectors) were placed equi-distant from each other. Another approach to phase reading is to use non-uniform sampling by placing the samplers in any required arrangement giving a desired transmit beam shape and direction. This technique is useful when a special beam pattern is desired as in conformal arrays. For example, if the fibers are positioned such that the inter-fiber distance has a quadratic behavior along the sampling direction, the microwave signals have a phase that changes quadratically along the array, producing converging/focusing or diverging antenna beams.

8.2 Single Frequency Beam Azimuth/Height Control

The linear phased array optical processor can be used to steer an N X M element planar array beam in azimuth/height using one control frequency, although the azimuth and height coordinates are dependent on each other. As the control frequency is varied, the beam follows a specific path in azimuth/height coordinates, as shown by the curves in Fig.11(c). The N X M sampler locations along the linear slit of light are shown in Fig.11(a). Note that the sampler located at the linear coordinate $x=nd+m\Delta d$ drives the (m,n) element in the array, where m is the row number and n is the column number, respectively. d is the spacing between samplers feeding adjacent elements along a row of the array antennas. Δd is the sampler separation in the N sets of M samplers that feed the column elements of the planar array. Note that the phase shift between adjacent elements (m,n) and (m,n+1) is ψ, while for elements (m,n) and (m+1,n) is ψ/M, that is, M times smaller. This leads to a large angular deflection with frequency in one direction (with the large phase change), while a nearly M times smaller angular deflection in the orthogonal direction. This type of array feed format may be useful when a pencil beam with a wide scanning range in one direction and a small scan width in the orthogonal direction is required. For example, this type of feed is useful in the shuttle scanning strip-mode synthetic aperture radar where 23 degrees of azimuth coverage is required compared to 1 degree for height changes to account for earth curvature effects. Fig.11(b) shows the signal feed configuration on the planar N X M array antenna. Note that in the linear sampling format used for instance in Fig.1, the fibers/detectors are placed a certain distance apart. This implies that most of the light between any two adjacent fibers is wasted, making a some what inefficient system. One feature of the sampling format shown in Fig.11(a) is its efficient use of the available optical power.

8.3 Simultaneous Dual Symmetric Beam Scanning

For a scan control frequency f corresponding to a beam scan angle θ, signals provided by the linear phased array optical processor can be distributed to the individual antennas such that two symmetric, simultaneous beams can be generated at positions θ and $-\theta$. Thus, by varying the control frequency f, the two beams can be rotated symmetrically around the broadside position. The linear array processor in Fig.1 is altered by placing a 50:50 beam splitter before the output detector sampling plane creating two output ports. The phase sampling along one output port is done in the x direction, while at the other output port, the sampling is done along the -x direction. This sampling approach generates two sets of signals that are phase conjugates of each other.

9. Features of the AO Technique

The AO antenna control architecture eliminates the large number of electronic phase shifters and their multiple control signals, along with extensive computer hardware and software systems. The optical phase control mechanism is independent of the antenna carrier frequency. This is unlike most conventional phase shift mechanisms, where a frequency dependent material parameter is used to introduce the phase shift. Intrapulse beam forming is easily possible, and frequency scanning can also be used for beam control. In addition, the basic in-line design can be made smaller using in-plane counterpropagating AODs (see Fig.12), although, at the cost of lower overall optical efficiency. The in-line additive architectures efficiently use the diffracted and undiffracted beams from the low (<10%) diffraction efficiency AODs to provide lower required optical power levels for the system. Table 1 gives a comparison of the optical efficiency of various architectures using a 10% diffraction efficiency for the AODs.

10. Conclusion

This paper has introduced phase based acousto-optic techniques for control and signal processing in linear and planar phased array antennas. 1-D and 2-D scanning architectures are described. In addition, there is the possibility of integrating the linear array architecture on a substrate using

surface acoustic wave (SAW) devices, thus leading to smaller and lighter phased array antenna systems.

11. Acknowledgements

The author would like to thank Demetri Psaltis at Caltech for useful discussions. The experiments were performed at Caltech with support from the AFOSR and AOSR.

12. References

[1] J. J. Pan, ``Fiber optics for wideband extra high frequency (EHF) phased arrays,'' SPIE Proc., Vol.886-08, Jan., 1988.
[2] G. A. Koepf, ``Optical processor for phased array antenna beam forming,'' SPIE Proc., Vol. 477, 1984.
[3] N. A. Riza and D. Psaltis, ``An acousto-optic technique for beam scanning and beam formation in phased array radars,'' OSA Annual Conf. Digest, No. 0127, Oct-Nov., Santa Clara, CA, 1988.
[4] N. A. Riza, ``Novel acousto-optic systems for spectrum analysis and phased array radar signal processing,'' Chapter 6, Ph.D Thesis, Caltech, Oct., 1989.
[5] M. L. Skolnik, Introduction to Radar Systems, Chapter 8, Copyright: McGraw-Hill, 1981.
[6] T. C. Cheston and J. Frank, Phased Array Radar Antennas, Ch. 7, Radar Handbook, Editor, M. I. Skolnik, 2nd Ed. McGraw Hill, New York, 1990.
[7] R. J. Mailloux, ``Phased array theory and technology,'' Proc. of the IEEE, Vol.70, No.3, March, 1982.
[8] L. B. Lambert, M. Arm, and A. Aimette, ``Electro-optical signal processors for phased array antennas,'' Chapter 38, Optical and Electo-Optical Information Processing, edited by J. T. Tippett et al., MIT Press, Cambridge, MA, 1965.
[9] R. G. Rosemeier, J. I. Soos, and J. Rosenbaum, ``A single element 2-D acousto-optic GaP laser beam steerer,'' SPIE Proc., No. 898-07, 1988.

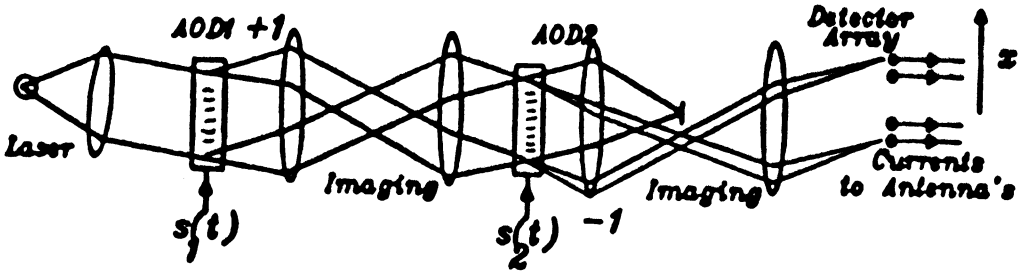

Fig.1 The basic in-line additive AO Architecture for a linear phased array.

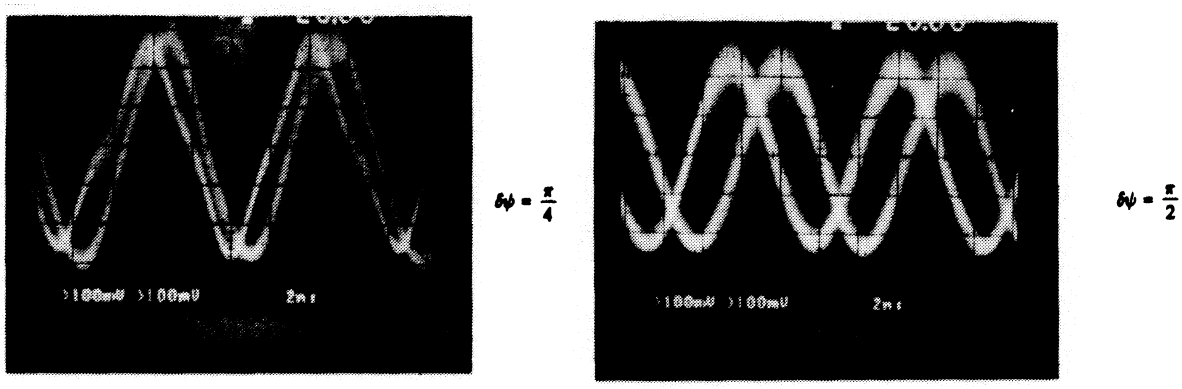

Fig.2 Oscilloscope traces of two phase shifted signals from the AO processor.

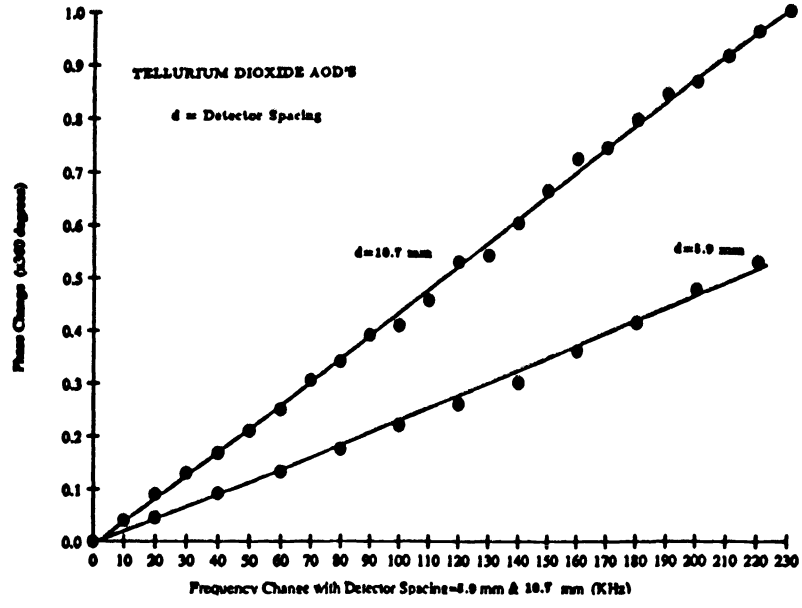

Fig.3 Experimental plot of Signal Phase Change .vs. Control Frequency Change.

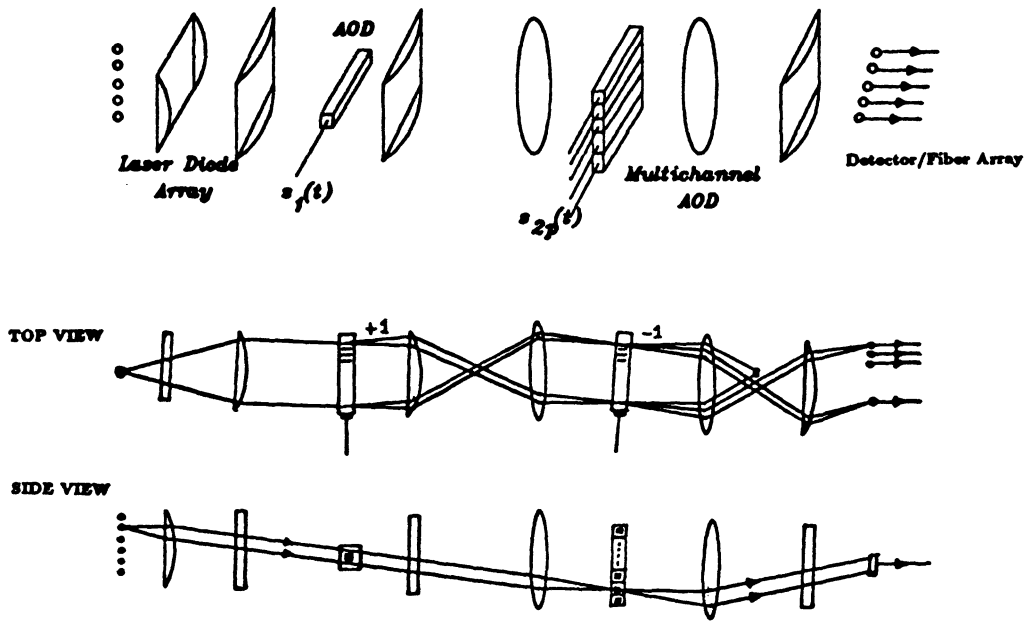

Fig.4 Simultaneous Multiple Beam Forming AO Architecture.

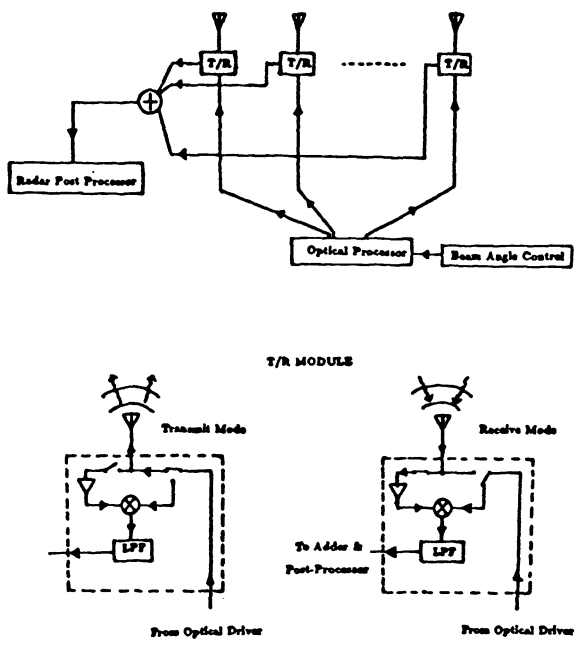

Fig.5 Electronic Receive Technique.

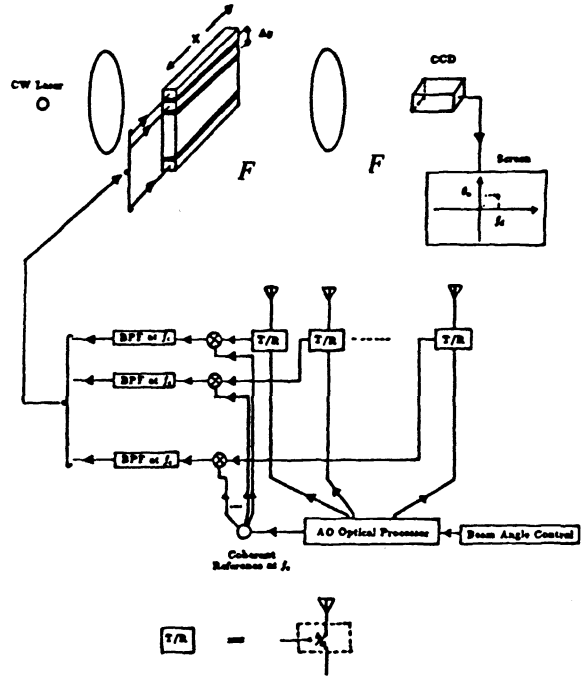

Fig.6 Optical Receive Technique.

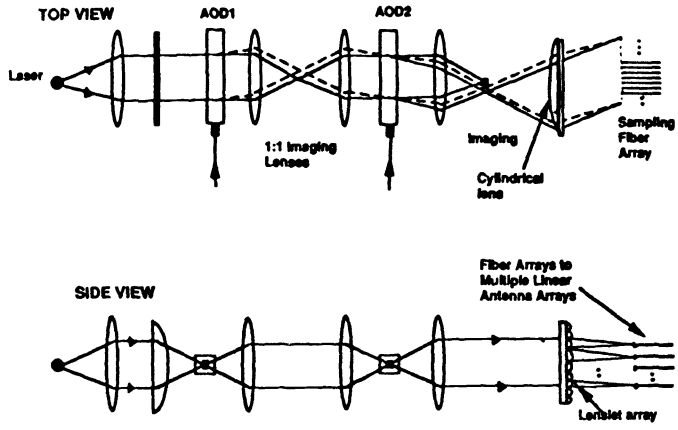

Fig.7 Multiple Linear Array Feed Architecture for 1-D Scanning.

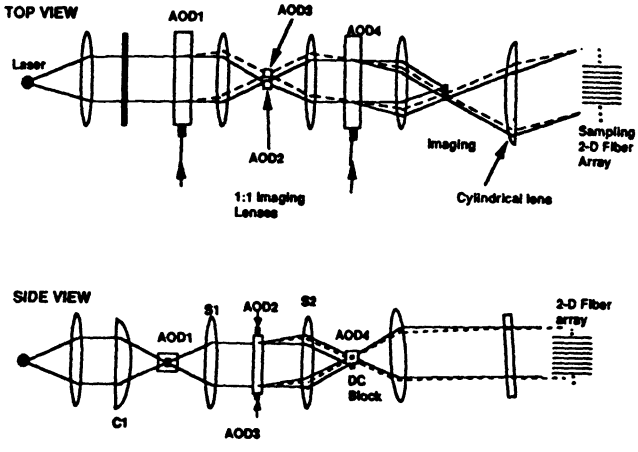

Fig.8 In-line Architecture for 2-D Scanning using 4 1-D AODs.

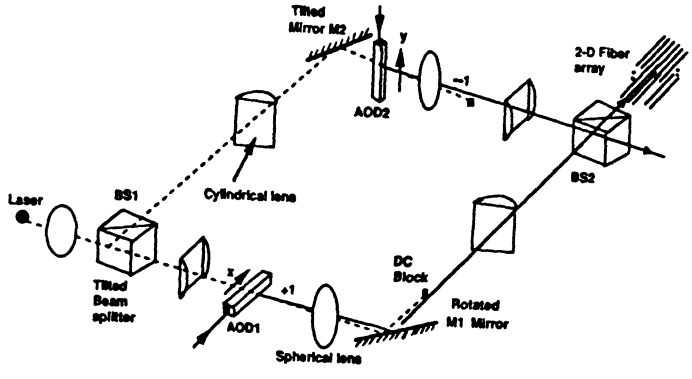

Fig.9 Mach-Zehnder Architecture for 2-D Scanning using 2 1-D AODs.

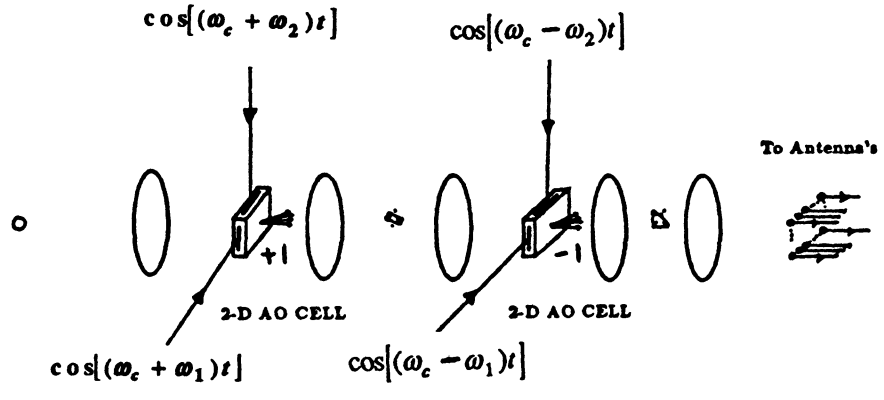

Fig.10 In-line Architecture for 2-D Scanning using two 2-D AO cells.

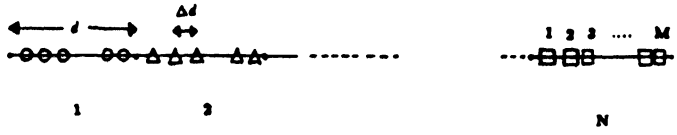

a): Sampler Distribution Along Linear Phase Pattern

b): Planar $N \times M$ Array Current Feed Configuration

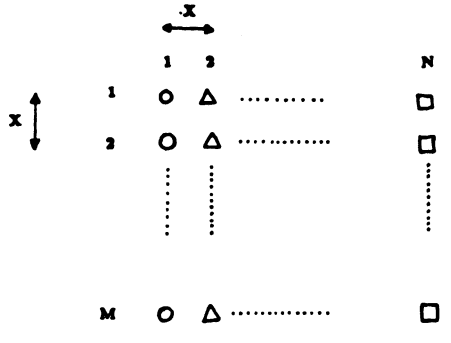

c): Beam Scan Path in Space

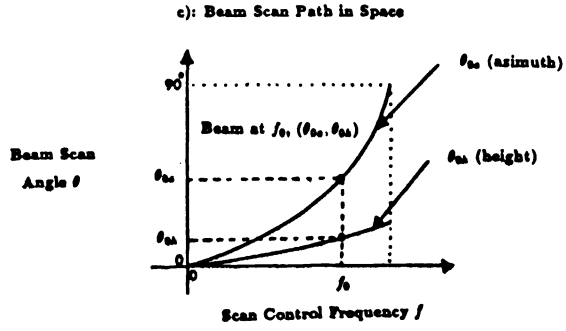

Fig.11 Single Control Frequency Coupled 2-D Scanning Technique.

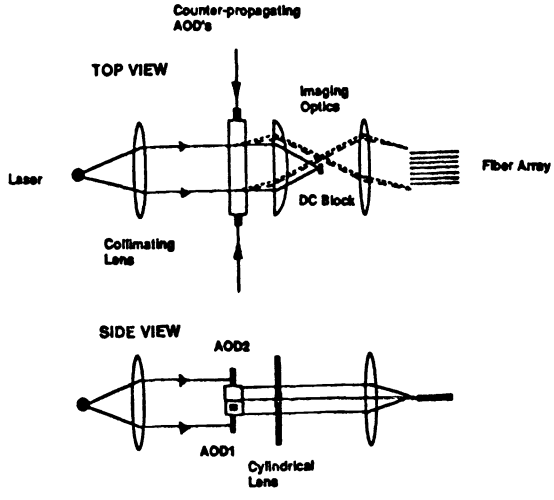

Fig.12 Compact In-line Architecture for a linear array.

ARCHITECTURE	Optical Efficiency
Basic in-line additive 1-D Scanning (Fig.1)	~ 20 %
Counter-propagating AODs 1-D Scanning (Fig.12)	~ 10 %
In-line 4 AODs 2-D Scanning (Fig.8)	~ 2 %
Mach-Zehnder 2 AODs 2-D Scanning (Fig.9)	~ 5 %

Table.1 Comparison of Optical Efficiency for different AO Architectures.